Role of recording geometry in the performance of spectral diversity filters with spherical beam volume holograms

Chaoray Hsieh, Omid Momtahan, Arash Karbaschi, and Ali Adibi

School of Electrical and Computer Engineering, Georgia Institute of Technology, Atlanta, Georgia 30332

Michael E. Sullivan and David J. Brady

Department of Electrical and Computer Engineering, Duke University, Durham, South Carolina 27708

Received May 18, 2004

We present experimental demonstrations of spectral diversity filters with spherical beam volume holograms for multimodal multiplex spectroscopy. Major properties of filters under diffuse-light illumination are discussed. The comparisons of spectral diversity between the transmission geometry holograms and the reflection geometry holograms are also studied. The results show that there is a trade-off between the degree of the spatial coherence of the source and the spectral diversity of the filter. We also conclude that the reflection geometry holograms have better spectral diversity and less sensitivity to the spatial coherence of the source. © 2005 Optical Society of America

OCIS codes: 090.7330, 300.6300.

Compact and sensitive spectrometers are of high utility in biological and environmental sensing. Wavelength channels in a conventional spectrometer are separated by gratings, cavities, and interferometers. Although conventional devices efficiently separate multiple wavelength channels of a spatially coherent (or collimated) incident beam, their direct application for spatially incoherent beams is not trivial. A spatially incoherent beam has multiple spatial modes, which can be considered as different incident angles, resulting in the spatial overlap of multiple wavelength channels in the output plane of the grating. To suppress this ambiguity in the output spectrum, spatial filters (usually in the form of one or a few slits) are used in a conventional spectrometer to limit the incident light to one spatial mode, resulting in the detection of only one wavelength channel. Rotating the grating allows different wavelength channels to be analyzed. The main drawback of this single-mode single-channel scheme is the low optical throughput. For sensing applications in which the information-bearing signal is weak, more-sensitive schemes must be implemented. The idea of multimodal multiplex spectroscopy (MMS) was recently proposed based on using a weighted projection of multiple wavelength channels (i.e., multiplex) and combining several spatial modes (i.e., multimodal) of the incident signal.[1] In the formulation of MMS, the spectral diversity filler (SDF) is represented as a transfer function matrix (i.e., $\overline{\overline{H}}$), measured with a set of calibration monochromatic light sources.[1] Measuring the output pattern (i.e., m) corresponding to any input spectrum (i.e., s) allows the unknown spectrum to be estimated by a conventional optimization technique such as nonnegative least mean squares (i.e., $\min_s ||\overline{\overline{H}}s - m||_2$).[1] The original demonstration of MMS was based on using an inhomogeneous three-dimensional (3D) photonic crystal SDF.[1] However, fabrication of arbitrary inhomogeneous 3D photonic crystals is complicated. As a more reliable alternative, we recently proposed volume holographic SDFs.[2] In this Letter we explain the spectral properties of SDFs made by a simple spherical beam volume hologram (SBVH) and discuss the effect of recording geometry on the performance.

The SDF studied in this Letter is a SBVH recorded by a plane wave and a spherical wave generated by focusing another plane wave by use of a lens with a numerical aperture NA of 0.25. Figure 1(a) shows the recording setup for a transmission geometry SBVH. For a reflection geometry hologram the point source is placed behind the recording material, which is an $L = 200$ μm thick sample of Aprilis photopolymer.[3] The recording wavelength is 532 nm, and the hologram covers a 3.5 mm $\times$ 3.5 mm area of the recording material. Figure 1(b) shows the setup for measuring the transmitted spectrum of the holographic SDF. The

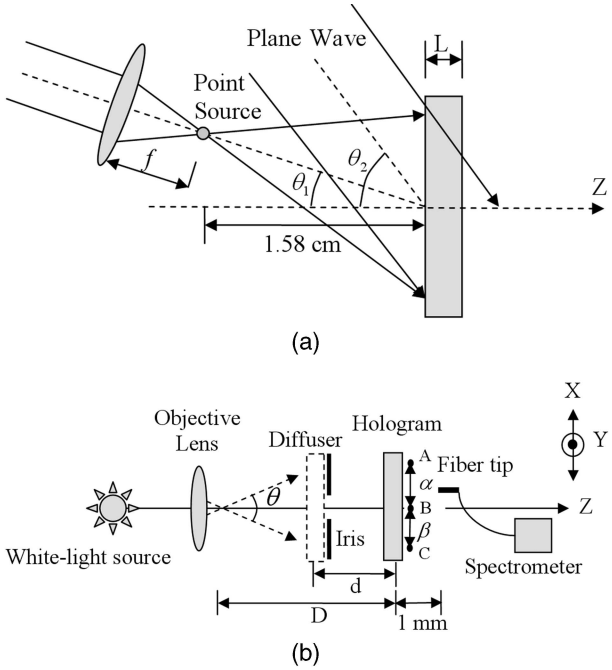

Fig. 1. Setup for (a) recording transmission geometry hologram and (b) measuring the transmitted spectrum of the holographic SDF.

0146-9592/05/020186-03$15.00/0

white-light source is a 50-W halogen bulb, and an objective lens (NA = 0.65) is used to produce a point source with an effective divergence angle θ that can be adjusted by changing the distance D between the point source and the hologram due to the limited size of the hologram compared with the size of the incident spherical beam. The lamp and the objective lens are both mounted on an $x-y$ stage so that the position of the point source can be shifted in both in-plane (x) and out-of-plane (y) directions, where the plane is formed by the two recording beams. A similar setup is used for reflection geometry holograms with the setup for forming the reading beam placed behind the hologram. A rotating diffuser can be added to the system for investigating the performance of the SDF for spatially incoherent incident beams. The size of the diffuser and the distance between the diffuser and the hologram (d) can also be controlled. A fiber tip [SMA 905 single-strand optical fiber (NA = 0.22)] connected to an Ocean Optics USB2000 spectrometer is located 1 mm behind the hologram to measure the transmitted spectrum at different locations in the output plane. Figure 2 shows the transmitted spectrum at three different locations [specified by A, B, and C in Fig. 1(b)] in the output plane of a transmission geometry hologram. The transmission dip at each location is the result of the diffraction of the incident light by the hologram. The bandwidth of the transmission dip (which is defined by the difference between the wavelengths corresponding to the two edges of the dip) corresponds to the wavelength selectivity of the hologram. Figure 2 shows that, when the fiber tip moves from point A to point C, the center wavelength of the transmission dip moves from 515 to 673 nm. This dependence of the transmitted wavelength on the location in the output plane shows that good spectral diversity can be obtained from SBVHs. Note that the results shown in Fig. 2 were obtained without putting the diffuser into the system.

The performance of the holographic SDF under diffuse light can be studied by putting a rotating diffuser (which is a sandblasted plastic plate) into the setup in Fig. 1(b). After adding the diffuser at a distance of d = 15.5 cm from the hologram, we repeated these measurements for both transmission and reflection geometry holograms, and the results are shown in Figs. 3(a) and 3(b), respectively. For the transmission geometry hologram, as shown in Fig. 3(a), the bandwidth of the transmission dip becomes larger and the strength of this dip becomes considerably smaller. This implies weaker spectral diversity of the filter for diffuse light. On the other hand, as shown in Fig. 3(b), a much-smaller bandwidth of the transmission dip is obtained for the reflection geometry hologram. Moreover, both the bandwidth and the strength of the transmission dip are almost not affected by the diffuse light. Therefore the reflection geometry can not only provide much-better wavelength selectivity (which agrees with the conventional theory of holograms[4]) but also holds excellent spectral diversity even under diffuse-light illumination. To further investigate the effect of the spatial coherence of the reading beam, we read the

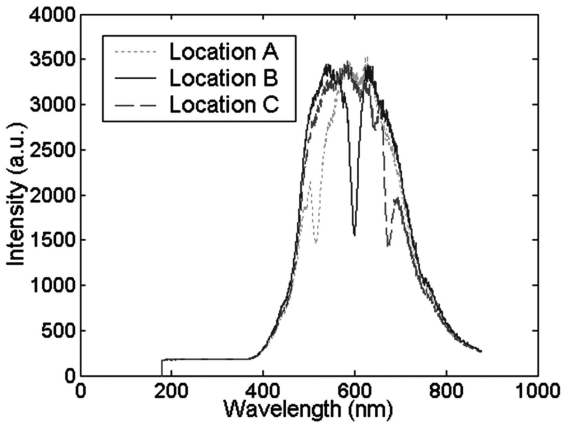

Fig. 2. Transmitted spectrum at three different locations A, B, and C [specified in Fig. 1(b) with D = 8 cm (which is chosen arbitrarily), $\alpha = \beta$ = 1.2 mm, and no diffuser present] on the output plane of the transmission geometry hologram.

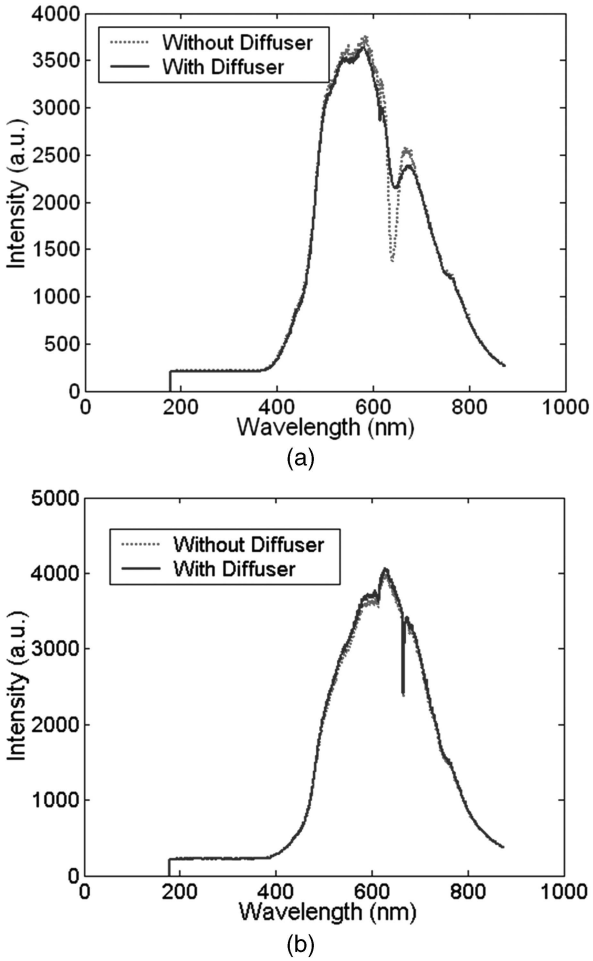

Fig. 3. Effect of the diffuser on the transmitted spectrum for (a) transmission geometry holograms and (b) reflection geometry holograms both measured between points B and C in Fig. 1(b) with D = 16 cm. The diffuser is located at d = 15.5 cm in front of the holograms. D and d are chosen large enough to clearly show the effect of the diffuser. The difference between the strengths and the widths of the transmission dips for the two recording geometries is clear. Similar behavior exists at other output points such as B and C.

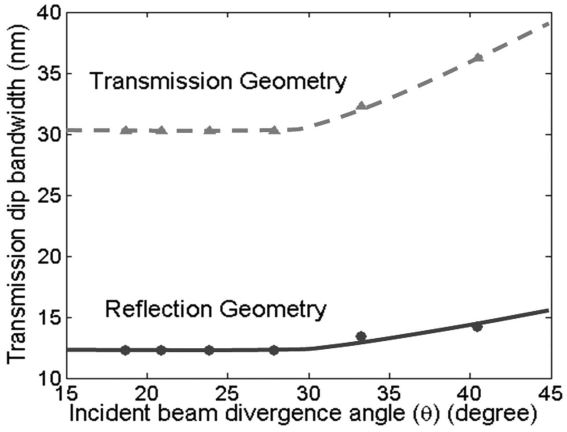

Fig. 4. Effect of the incident beam divergence angle on the bandwidth of the transmission dip. With no diffuser present, the divergence angle of the incident beam is modified by changing D in Fig. 1(b). The measurement is made at point C shown in Fig. 1(b).

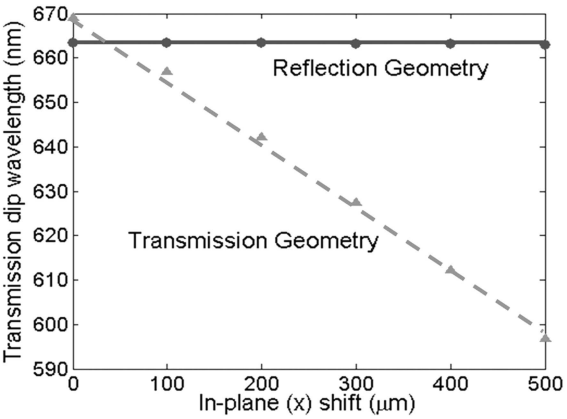

Fig. 5. Effect of in-plane (x) shift of the reading point source on the transmission dip wavelength for transmission geometry holograms and reflection geometry holograms. The distance between the point source and the hologram is $D = 0.93$ cm, and the diffuser is removed from the setup in Fig. 1(b). D is chosen small enough to obtain a practical range for in-plane (x) shift. The measurement is made at point C shown in Fig. 1(b).

holograms with a diverging beam (generated by focusing a plane wave) with different divergence angles [the diffuser is taken out of the setup in Fig. 1(b)]. The variation of the transmission dip bandwidth with the divergence angle of the incident beam is shown in Fig. 4. Figure 4 also shows that increasing the divergence angle in the transmission geometry causes the dip bandwidth to become larger, and it increases by 30% for $\theta = 45°$. Although a similar behavior is seen for the reflection geometry hologram, much less increase in the dip bandwidth is observed. We also studied the strength of the transmission dip and found that, for the transmission geometry hologram, the strength of the dip decreases by 25% as divergence angle θ is increased to 45°, whereas the dip strength is almost unaffected (less than 5% decrease) for the reflection geometry hologram as θ is increased to 45°. Note that by limiting the divergence angle of an arbitrary incoherent source, we limited the total optical power that illuminates the hologram. Thus the results shown in Fig. 4 suggest that there is a trade-off between the available optical power for illumination (or the degree of spatial coherence) and the spectral diversity of the holographic SDFs. This trade-off is much stronger in transmission geometry, in which a 45° divergence angle might be the reasonable upper bound (see Fig. 4). The results shown in Fig. 4 suggest that (when the design criteria allow) reflection geometry holograms are better candidates for the implementation of SDFs. Besides the larger wavelength selectivity[4] of these holograms (compared with transmission geometry), their lower shift selectivity[5,6] is another reason for their excellent spectral diversity. This is shown in Fig. 5, which depicts the variation of the center wavelength of the transmission dip (for both recording geometries) with the in-plane shift (x) of the reading point source. It is clear from Fig. 5 that the transmission dip from different input points occurs at different wavelengths in transmission geometry. Thus, for a spatially incoherent source (which can be considered as a combination of an array of incoherent point sources in the input plane), the combination of all these dips results in a wide and weak transmission dip as seen in Fig. 3(a). On the other hand, the transmission dip wavelength is not modified considerably with the in-plane shift (x) in reflection geometry. As a result, the properties of the transmission dip are not strongly affected by use of a spatially incoherent source as Figs. 3 and 4 suggest. Although not shown here, out-of-plane shift (y) results in a similar variation for the transmission dip wavelength with the position of the input source.

In conclusion, we have presented quantitative experimental evidence for the feasibility of using SBVHs as SDFs for MMS. We have shown that there is a trade-off between the degree of the spatial coherence of the source and the spectral diversity of the filter. We have also shown that reflection geometry holograms have better spectral diversity and less sensitivity to the spatial coherence of the source than transmission geometry holograms.

This work was supported by the National Institutes of Health and by the David and Lucile Packard Foundation. A. Adibi's e-mail address is adibi@ece.gatech.edu.

References

1. Z. Xu, Z. Wang, M. E. Sullivan, D. J. Brady, S. H. Foulger, and A. Adibi, Opt. Express **11,** 2126 (2003), http://www.opticsexpress.org.
2. A. Karbaschi, C. Hsieh, O. Momtahan, A. Adibi, M. E. Sullivan, and D. J. Brady, Opt. Express **12,** 3018 (2004), http://www.opticsexpress.org.
3. H. J. Coufal, D. Psaltis, and G. T. Sincerbox, eds., *Holographic Data Storage* (Springer-Verlag, New York, 2000), pp. 171–197.
4. D. Psaltis and F. Mok, Sci. Am. **273,** 70 (1995).
5. G. Barbastathis and D. Brady, Proc. IEEE **87,** 2098 (1999).
6. G. Barbastathis, M. Levene, and D. Psaltis, Appl. Opt. **35,** 2403 (1996).